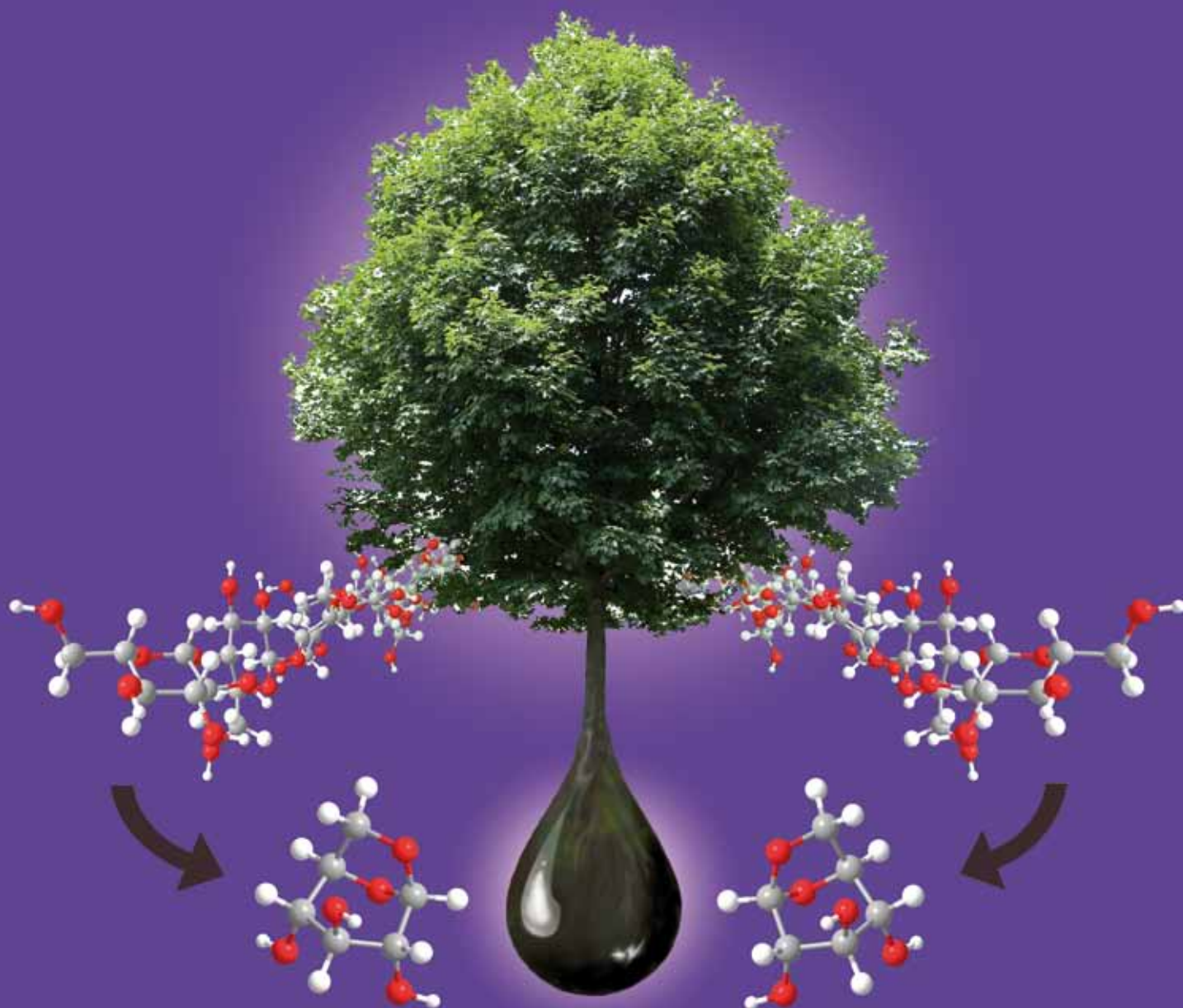


Green Chemistry

Cutting-edge research for a greener sustainable future

www.rsc.org/greenchem

Volume 11 | Number 10 | October 2009 | Pages 1485–1704



ISSN 1463-9262

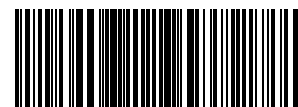
RSC Publishing

Abbott *et al.*
Probing gas expanded liquids

Dauenhauer *et al.*
Reactive boiling of cellulose for catalysis

Patel *et al.*
One pot preparation of cyanamide

Chen *et al.*
Facile preparation of Pd/organoclay catalysts



1463-9262(2009)11:10;1-A

Reactive boiling of cellulose for integrated catalysis through an intermediate liquid†

Paul J. Dauenhauer,^{‡a} Joshua L. Colby,^a Christine M. Balonek,^a Wieslaw J. Suszynski^b and Lanny D. Schmidt^{*a}

Received 11th May 2009, Accepted 23rd July 2009

First published as an Advance Article on the web 14th August 2009

DOI: 10.1039/b915068b

Advanced biomass processing technology integrating fast pyrolysis and inorganic catalysis requires an improved understanding of the thermal decomposition of biopolymers in contact with porous catalytic surfaces. High speed photography (1000 frames per second) reveals that direct impingement of microcrystalline cellulose particles (300 μm) with rhodium-based reforming catalysts at high temperature (700 °C) produces an intermediate liquid phase that reactively boils to vapors. The intermediate liquid maintains contact with the porous surface permitting high heat transfer (MW m^{-2}) generating an internal thermal gradient visible within the particle as a propagating wave of solid to liquid conversion. Complete conversion to liquid yields a fluid droplet on the catalyst surface exhibiting a linear decrease in droplet volume with time leaving behind a clean surface absent of solid residue (char). Under specific interfacial conditions, conversion with large cellulosic particles on the length-scale of wood chips (millimeters) occurs continuously as generated liquid and vapors are pushed into the porous surface.

Introduction

The search for advanced processing technologies capable of efficiently converting biomass to fuels and chemicals has led to the combination of solid biomass pyrolysis and catalytic processes. Direct utilization of catalysts with biomass requires the large biopolymers of lignocellulose to be broken down to species capable of interacting with catalytic active sites while maintaining catalyst integrity.¹ Emerging technologies have shown that high temperature decomposition (*e.g.* fast pyrolysis) pairs well with the use of inorganic catalysts due to similar processing rates, occurring orders of magnitude faster than existing biological processes (*e.g.* enzymatic hydrolysis).^{2–4} Recently, Huber *et al.* demonstrated mixed pyrolysis/catalysis by rapid heating of cellulose particles in the presence of aluminosilicates (*e.g.* ZSM-5), which both cracked large biopolymers and converted the organic intermediates to highly desirable gasoline-like aromatic species.⁵ Additionally, Schmidt *et al.* demonstrated that alumina-supported reforming catalysts combined with cellulose pyrolysis efficiently produce synthesis gas ($\text{H}_2 + \text{CO}$) and allow for selective tuning of product ratios.^{6,7}

However, the mechanism by which cellulose thermally decomposes to volatile organic compounds (VOCs) on catalytic surfaces for downstream processing is unknown, hindering advancement of catalytic biomass reactors. The process generally occurs by cellulose particles impacting a high temperature surface, driving endothermic pyrolysis of the polymer structure to VOCs. These products are then convected from the particle to the neighboring solid, interacting chemically with the catalyst surface. Unknowns within this complex set of interacting phenomena are the dominant method of heat transfer to particles (convection, radiation, or conduction), the state of the cellulose particle over the course of conversion (solid or liquid), the extent of particle homogeneity, the physical interaction between the particle and surface, and the rate limiting phenomenon (pyrolysis or some mode of heat transfer). The complex nature of the system prevents substantial understanding by transport models integrating particle, surrounding gas, and surface chemistry.

This paper examines the conversion of cellulose particles in direct contact with high-temperature catalytic reforming catalysts in the presence of oxygen. Small, pure particles of cellulose on the length scale of 10–400 μm are observable under significant optical and temporal magnification (1000 frames per second). Variation of the catalytic surface between realistic porous foam supports and experimental flat surfaces permits a clear observation of the particle/surface interaction. Additionally, dimensional tracking of particles with time reveals the extent of conversion from solid cellulose to intermediate phases, and it permits an indirect measurement of surface-to-particle heat transfer.

The results show that micron- to millimeter-scale particles decompose to an intermediate liquid droplet before further decomposing and boiling completely to volatile species. The

^aDepartment of Chemical Engineering and Materials Science, University of Minnesota, 421 Washington Ave S.E., Minneapolis, MN 55455, USA. E-mail: schmi001@umn.edu; Fax: 612/625-1313; Tel: 612/625-9391

^bCoating Process Fundamentals Visualization Laboratory, University of Minnesota, 421 Washington Ave S.E., Minneapolis, MN 55455, USA. E-mail: suszy001@umn.edu

† Electronic supplementary information (ESI) available: The supplementary information consists of one summary of methods and supplementary figures and four videos obtained from high speed photography. See DOI: 10.1039/b915068b

‡ Present address: University of Massachusetts, Amherst. E-mail: dauenhauer@ecs.umass.edu

intermediate particle predominately exists as a heterogeneous mixture of solid and liquid with linear reduction in height with respect to time indicating a potential for continuous processing of larger particles. Therefore, additional experiments consider high temperature reforming catalysts in contact with large particles (rods, $7 \times 7 \times 500$ mm) that extend away from the surface permitting examination of continuous catalytic processing of cellulose. The processing rate was measured as a function of the interfacial temperature and the applied pressure between the cellulose feedstock and the catalytic surface.

Experimental

Catalytic reforming of cellulose particles was examined in three separate experimental apparatuses due to the significant difference in cellulose feedstock dimensions (micron- *versus* centimeter-scale) and catalyst supports (foam *versus* flat surfaces).

Catalyst preparation

The catalyst in Fig. 1a was supported on an 80 pores per inch (ppi) α -Al₂O₃ foam cylinder 17 mm in diameter and 10 mm in length with visible struts and tortuous pores. The flat catalytic surface (wafer) in Fig. 1b was prepared by compressing α -Al₂O₃ powder into a disk 2 mm thick and 22 mm wide, sintering at 800 °C for 30 hrs and 1180 °C for 8 hrs. Both catalysts were prepared by wet impregnation of Rh-Ce (2.5 wt% of the support each), drying, and calcination at 600 °C for 6 hrs.

Micron-scale particle processing on foam supports

Small particle (<500 μ m) autothermal conversion was examined in a 20 mm I.D. quartz reactor tube described previously.⁶ Three foams were stacked on top of each other along with a fourth blank 80 ppi foam on the bottom, wrapped in ceramic paper (for friction fit), and slid into the reactor tube. A type K thermocouple was inserted 10 mm from the leading surface. A 1 cm pyrex tube combined with a size 20 pyrex reactor tube end cap provided the connection between the reactor and a cellulose hopper necessary for solid particle delivery. A quartz light pipe was inserted through the end cap and contacted the leading surface providing a light sample to an optical pyrometer. The cellulose particles (avg. 315 μ m) stored in an acrylic tube hopper (~10 cm diameter) were pushed into a feed tube (0.25 inch I.D.) using a 0.25 inch wood auger driven in reverse with a servo motor permitting variable feed rates. Air was supplied by a gas cylinder and metered by a flow control valve calibrated with a bubble column.

The quartz reactor was wrapped in a resistive heater controlled by a variac and wrapped in insulation. Autothermal operation was initiated with air flow of 1.5 standard liters per minute (SLPM) by heating the reactor externally to ~400 °C at which point particles were continuously delivered to the surface. Steady autothermal operation was obtained within five minutes, and the heater was turned off. Varying surface temperatures were obtained by varying the air flow rate or cellulose flow rate. The high speed camera was placed ~45° from the surface normal, obtaining light through the curved quartz reactor wall. Light for high-speed photography was provided to the front of the

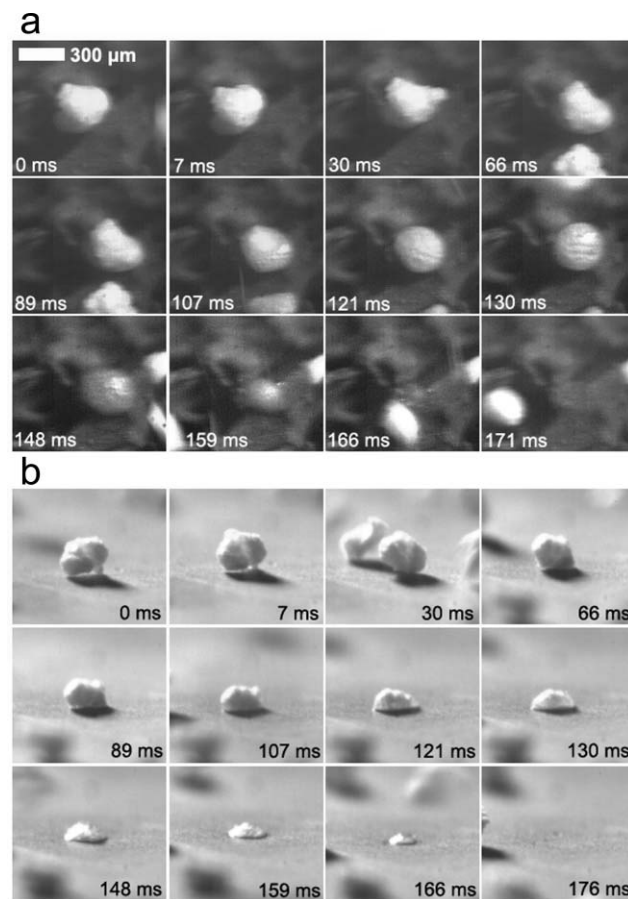


Fig. 1 Millisecond visualization of cellulose particle decomposition. **a**, Microcrystalline cellulose particles (~300 μ m) reacting to form volatile species in air on 700 °C Rh-Ce/ α -Al₂O₃ have been visualized with high-speed photography (1000 frames/second) on an 80 ppi α -Al₂O₃ foam support at C/O = 1.15. **b**, A separate experiment examined cellulose decomposition on a smooth 700 °C Rh-Ce/ α -Al₂O₃ disk support. Particles exhibit poor surface contact (0–7 ms) before forming a liquid intermediate species capable of intimately contacting the catalytic surface (66–176 ms). The molten intermediate liquid appears to nucleate volatile species (107–130 ms) before completely converting without char formation (171–176 ms).

particles. Figure S1 of the supplementary information depicts the experimental setup.†

Micron-scale particle processing on flat supports

Particles of cellulose and sucrose pyrolyzing on a flat catalytic wafer (Rh-Ce/ α -Al₂O₃, 2.5 wt% each) were observed using a high speed camera. A quartz reactor tube was fixed in place 1–2 cm above the catalytic wafer by metal clamps. Air was supplied by a high pressure gas cylinder through a needle valve, and particles of solid material were applied down the reactor tube to the catalytic surface from a side tube sealed with a pushrod. A quartz fiber light pipe delivering light to an optical pyrometer was attached through the quartz reactor such that it contacted the catalytic surface. A butane torch was clamped directly below the catalytic wafer such that its distance was adjustable to control the surface temperature. The high speed

camera was placed $\sim 80^\circ$ from the surface normal, obtaining light through a flat pyrex protector plate. Light for high-speed photography was provided from behind the particles. Figure S9 of the supplementary information depicts the experimental setup.†

Centimeter-scale particle processing

Large particles of cellulose ($7 \times 7 \times 500$ mm) were prepared by pulping a mixture of mainly hemicellulose and cellulose (79.8% glucan, 19.5% xylan, 0.3% lignin, 0.4% ash) in deionized water, drying the pulp in a mold ($50 \times 50 \times 1$ cm), and cutting the dried block to the desired dimensions.

Processing of large particles occurred on catalytic foams in a 20 mm I.D. reactor described above with the addition of a 1 cm I.D. pyrex tube extending ~ 1 m from the top of the reactor. Cellulose rods were pressed against the catalytic foam from above by weights placed within the sealed tube. The bulk surface temperature was varied from ~ 600 – 900 °C by varying the dilution of methane and oxygen feed gas with the constraint that $C/O = (\text{fuel C})/(\text{atomic oxygen from } O_2) = 0.8$ and total gaseous flow rate was 5.0 SLPM. Gaseous reactor effluent was collected and measured by gas chromatography to validate rod conversion rates. Figure S18 of the supplementary information depicts the experimental setup.†

Experiments were setup such that a rod of cellulose, 500 mm in length, was suspended 5 cm above the foam catalysts by a pin extending out of the reactor through a sealed port. Nitrogen, oxygen and methane, flowing around the suspended cellulose and through the catalyst, were heated by an external torch applied to the reactor wall near the catalyst to initiate autothermal reforming. The experiment was initiated by removing the pin permitting the cellulose rod to fall to the catalyst surface while simultaneously adjusting the oxygen/nitrogen/methane flow rates to satisfy $C/O = 0.8$. The rate at which the cellulose sample ablated on the catalyst was measured by recording the movement of the cellulose end as it passed graduations on the feed tube with time. Downstream gas samples were collected and analyzed by gas chromatography for carbon monoxide and carbon dioxide to verify carbon processing rates.

High-speed photography

Digital video was obtained by focusing a Photron Fastcam Ultima APX with color image through a curved quartz reactor or pyrex plate. The four optical devices placed in series to obtain the presented magnification were: 1) a Micro-NIKKOR 105 mm lens by Nikon of Japan, 2) a Nikon PN-11 extension tube by Nikon of Japan, 3) a Kenko extension tube for Nikon/AF 36 mm by Kenko of Japan, and 4) a Kenko 2x Teleplus MC7 telephoto extension tube by Kenko of Japan. Light was provided to the catalyst necessary for high speed imaging by a Solarc Light LB-50 by Welch Allyn, Inc. of New York, USA.

Visualization videos of particle conversion on catalytic foams were collected through the 2 mm thick quartz reactor tube, while particles on wafers were obtained through 0.5 cm pyrex glass used to protect the camera. Particle sizes were obtained by relating the measured number of pixels within a frame

to known sizes of objects (thermocouple or quartz light pipe).

Results and discussion

In the integrated pyrolysis/catalysis process examined here, particles of cellulose in air impact a glowing (~ 700 °C) Rh-Ce/ α -Al₂O₃ foam catalyst in a quartz reactor tube and pyrolyze completely under extreme thermal gradients to VOCs at millisecond time-scales. The VOCs flow into the catalyst, react with oxygen exothermically, and generate sufficient heat to maintain the catalyst at 700 – 800 °C driving endothermic pyrolysis in an overall exothermic, autothermal process.⁶ This arrangement has been shown to efficiently produce equilibrium selectivity to clean synthesis gas without detectable char formation.⁷

Through the use of ultra high-speed imaging (1000 frames per second) we definitively demonstrate the existence of a liquid intermediate during the rapid heating of cellulose particles. Fig. 1a shows the conversion of a single ~ 300 μ m diameter cellulose particle on an operating foam catalyst at ~ 700 °C from $\sim 45^\circ$ relative to the catalyst surface. After coming to rest on the surface (0 ms), the particle appears to initially rotate (7 & 30 ms) before the appearance of a smooth liquid layer along the bottom right edge (66 ms) distinguishable by its specular highlight. The development of a liquid phase continues to progress from the bottom of the particle (89 & 107 ms) until the entire particle exists as a hemispherical liquid droplet (121 ms). Clearly visible within the liquid layer are gaseous bubbles developing within the liquid sphere (107, 121, and 130 ms) moving to the surface and eventually the surrounding gas until the entire particle volatilizes leaving a clean surface (171 ms). All frames are available as supplementary video 1.†

In a different experiment (Fig. 1b) we examined the impact of cellulose particles in air on a flat Rh-Ce/ α -Al₂O₃ surface heated from below by a butane torch to 700 °C. Viewed at 80° from the surface normal, the particle initially exhibits poor surface contact (0–7 ms) before forming a liquid clearly in intimate contact with the catalyst (66–107 ms). Conversion to a liquid at 130 ms produces a hemispherical shape, which fully volatilizes leaving a clean surface at 176 ms. All frames are available as supplementary video 3.†

The existence of a liquid intermediate from cellulose, often referred to as ‘active cellulose,’ has elicited controversy.^{8–11} Several multi-step cellulose decomposition mechanisms include an intermediate cellulose-like biopolymer of reduced degree of polymerization to fit empirical data.^{12–15} Further depolymerization and fragmentation to organic liquids (*e.g.* methanol, hydroxyacetaldehyde, levoglucosan) dominates around 500 °C in seconds, while higher temperatures favor gases (*e.g.* CO, H₂, CO₂) and lower temperatures favor dehydration chemistry to solid char. Previous evidence for depolymerized liquid intermediate formation was observed by showing that cellulose rods, similar to ice or meltable polymers, can be ablated on hot surfaces.¹⁶ A different set of experiments exposed small particles of cellulose to very short durations of applied heat and observed solid products with smooth surfaces, indicative of intermediate liquids.^{9,17} However, the present evidence clearly shows a liquid state forming spherical conformations and interacting with surfaces and other particles.†

Dimensional tracking of several particles (Fig. 2a) on the catalytic foam shows that the conversion time is directly proportional to the square of the initial particle diameter, even for particles as small as 100 μm . Furthermore, measurements shown in Fig. 2b (height and width) depict the lifetime of both particles in Fig. 1 and reveal three stages in particle volatilization. In region A, the particle exhibits poor surface contact and no apparent change in size. In region B, intermediate liquid formation propagates up the particle, coinciding with a nearly linear reduction in height. Finally, in region C, the liquid droplet undergoes further pyrolysis to gases and volatile organics, exhibiting constant decrease in width and volume as shown in Figure S13 of the supplementary information.†

The nature of the intermediate liquid has enormous implications on the rate of heat transfer from catalytic surfaces for thermal conversion of cellulosic materials. Particle pyrolysis is categorized in two ways, according to the dominant mode of heat transfer (internal or external) and the rate limiting phenomenon (chemical conversion by pyrolysis, product gas mass transfer or heat transfer).¹⁸ In this case, the thermal decomposition chemistry of cellulose above 400 °C is sufficiently fast to never be rate limiting for particles on the order of ten microns and larger.^{19,20} Additionally, the chemistry observed in Fig. 1 and the data in Fig. 2b clearly shows that solid to intermediate liquid conversion dominates the conversion time eliminating gas phase product mass transfer from being rate limiting. Therefore, conversion can only be limited by heat transfer to the particle by radiation, convection, conduction from the surface, or internal particle heat transfer (Fig. 2a).

The behavior of total conversion time as directly proportional to the square of the initial diameter has previously indicated internal heat transfer limitation, thereby requiring the ratio of external to internal heat transfer (described by the Biot number, $Bi = hD/k$) to be large ($Bi > 10$) where k is the thermal conductivity of cellulose, D is the particle diameter, and h is the external heat transfer coefficient.^{11,21} Neither maximum radiation, $\epsilon = 1$ and $T_{\text{inf}} = 700$ °C ($10^{-2} < Bi_{\text{radiation}} < 10^{-1}$), nor gas convection calculated from the Ranz and Marshall correlation ($Bi_{\text{convection}} \sim 1$) are sufficiently large to limit the system by internal particle heat transfer.²² External heat transfer from the surface by conduction can be estimated from

$$q_{\text{Conduction}} = \rho \frac{dV}{dt} \frac{\Delta H_{\text{pyrolysis}}}{A_{\text{Contact}}} = h_{\text{Conduction}} (\Delta T) \quad (1)$$

The volume of the liquid droplet, V , in each frame was calculated by assuming the droplet was a portion of a sphere as shown in Figure S12 of the supplementary information.† This method reveals that the change in volume, dV/dt , of the liquid droplet (Fig. 2, region C) is constant as shown in Figure S13 of the supplementary information.† By calculating dV/dt from ~ 200 measurements of several particles (Fig. 2, region C) and assuming $\Delta H_{\text{pyrolysis}} = 538$ kJ kg⁻¹, $\rho = 650$ kg m⁻³, the heat flow, $q_{\text{Conduction}}$, is 3.4 ± 0.2 MW m⁻² as shown by a histogram in the Fig. 2b inset of all experimental measurements.†²³ Further assuming the intermediate liquid is approximately the fusion temperature described by Lede (739 K), then $\Delta T \sim 200$ °C, and h_{surface} must be $(1.7 \pm 0.1) \times 10^4$ W m⁻² K⁻¹, satisfying $Bi \sim 10$ and concluding that surface heat transfer is overwhelming

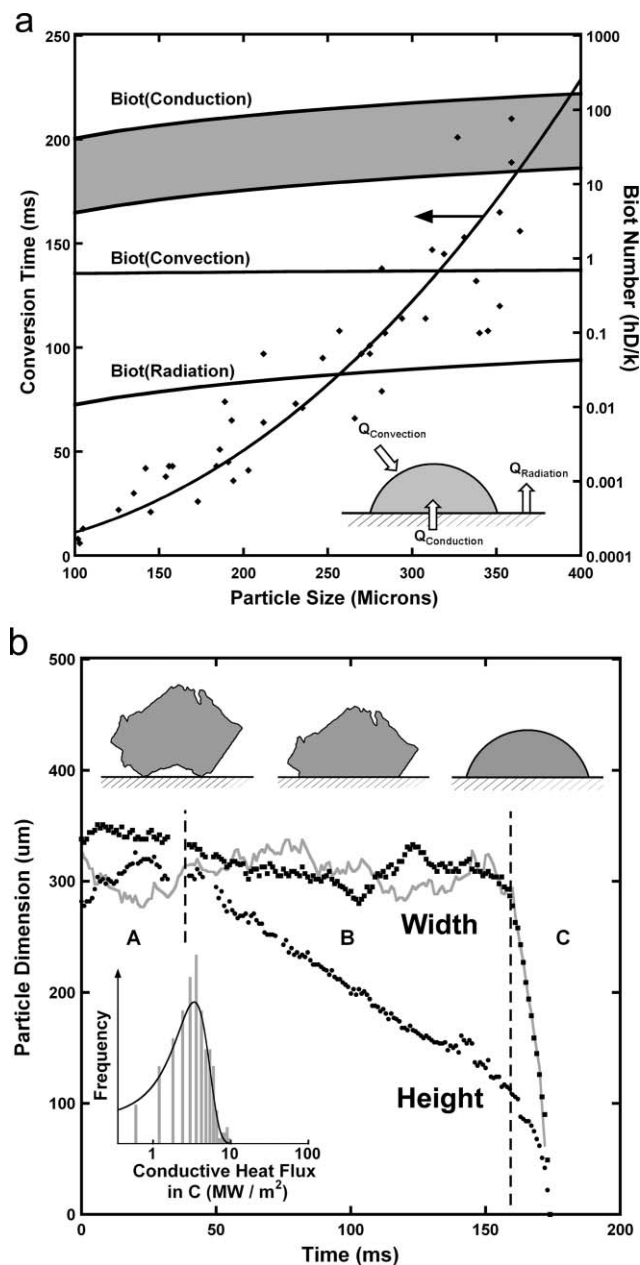


Fig. 2 Dimensional tracking of cellulose particle conversion for surface heat flux estimation. **a**, The time for observed particles to completely convert was proportional to the square of the initial particle diameter ($T_c = kD_o^2$) consistent with internal particle heat transfer control thereby requiring the ratio of external to internal heat transfer (Biot Number) to be larger than ~ 10 . Only a conductive heat transfer coefficient of $h = 10^4$ – 10^5 W m⁻² K⁻¹ (shaded region) can result in a Biot $\gg 1$ describing the thermal and reacting wave observed in Fig. 1. **b**, The conversion of a single cellulose particle (~ 300 μm) on a 700 °C surface appears to occur in three phases (A, B, and C) shown as a cartoon and described by height and width for flat surfaces (data points) and foams (grey line). (A) Initial impact with a catalytic surface exhibits very poor surface contact and slow initial heating. (B) Particle surface contact points eventually pyrolyze to a biopolymer liquid (active cellulose) which can contact the surface and permit rapid pyrolysis with a linear decrease in height. Gas nucleation was observed in the height around 140–150 ms. (C) An active cellulose drop exhibits linear decrease in volume (and radius of curvature) with time and an enormous heat flux of 3.4 ± 0.2 MW m⁻² (inset).

and dominant.¹⁶ Convection and radiation are included by this method of estimating the heat transfer rate, but their magnitude is on the order of the experimental error or less.

The mechanism permitting high conductive heat transfer to the particle can be observed in Fig. 1. Droplets of volatile fluids such as glycerol, heptane, or dodecane commonly exhibit film boiling (the Leidenfrost effect) which lift them off very hot surfaces, slowing conductive heat transfer.^{†24,25} However, experiments with cellulose (and additional experiments with sucrose available as video 4 in the supplementary information[†]) show that the liquid intermediate on a ~ 700 °C catalytic surface maintains contact, dramatically improving conductive heat transfer to the particle.

High heat flux through an intermediate liquid species has unique implications for the chemistry of cellulose decomposition. As observed in Fig. 1, cellulose conversion occurs as a thermal wave passing through the particle. For small particles considered here (< 500 μm), no portion of the particle exists sufficiently long at low temperature (~ 300 – 400 °C) for char-forming chemistry to occur appreciably. However, as a particle increases in size to 1 mm or greater (*e.g.* wood chips), it becomes unavoidable that a portion of the solid biopolymer away from the hot surface will exist within the char-producing temperature range. One demonstrated solution to this fundamental problem utilizes high heat transfer rates between a large (thermally-thick) particle and a hot non-catalytic surface moving relative to the sample to mechanically sweep away pyrolysis products.^{26–28} However, more simple processing of cellulose can occur with a stationary surface utilizing a catalyst on a porous surface.

A different experiment with cellulose (Fig. 3a) demonstrates that high heat flux through the liquid intermediate on catalytic surfaces can also process large rods ($7 \times 7 \times 500$ mm) rapidly. By pressing a cellulose rod directly onto a Rh-Ce/ Al_2O_3 foam co-forming methane, the rate of cellulose pyrolysis was measured as a function of applied pressure (12–36 kPa) and bulk catalyst surface temperature. Below a surface temperature of about 750 °C, the rod exhibited the expected behavior of intermediate char formation which permitted the rod to pass through the catalyst only as fast as the intermediate char gasification rate, ~ 50 $\text{kg m}^{-2} \text{hr}^{-1}$. However, above approximately 750 °C, the rod processing rate was considerably higher (> 300 $\text{kg m}^{-2} \text{hr}^{-1}$), linear in temperature, and a strong function of applied pressure, indicating that pyrolysis at the leading cellulose edge is the rate limiting step.²⁹

Fig. 3b describes a qualitative temperature distribution consistent with experimental observations. As heat flow from the surface (Q_{flux}) increases, the thermal gradient within the solid cellulose particle increases and the length of cellulose ('a' in Fig. 3b) existing within the char-forming temperature region decreases ('b' in Fig. 3b). At heat fluxes present in the described experiments, the thermal gradient within the cellulose rod is sufficiently steep to result in negligible char formation.

The decomposition of cellulose at the rod tip in contact with the catalytic surface likely undergoes very complex multiphase rearrangement. As solid cellulose decomposes to intermediate liquid, it is pushed into the pores of the catalyst. Additionally, individually developed fluid droplets are likely to coalesce to larger ones.

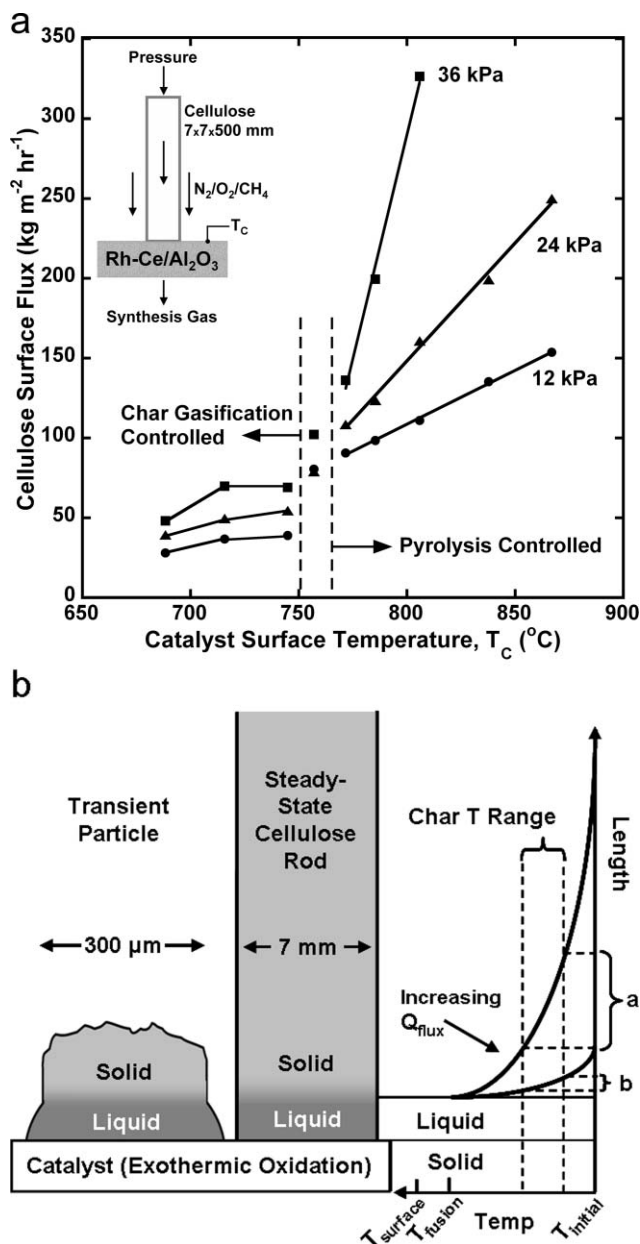


Fig. 3 Large particle conversion on catalytic surfaces. a, Cellulose particles ($7 \times 7 \times 500$ mm) reacted to synthesis gas on a Rh-Ce coated alumina foam by direct impingement in the presence of oxygen. The interface pressure was varied from 12–36 kPa, and the catalyst surface temperature was controlled by methane catalytic partial oxidation at $\text{C}/\text{O} = 0.8$ diluted with varying amounts of N_2 (total gas flow rate was a constant 5 SLPM). Cellulose conversion exhibited a distinct change in conversion rate (surface flux) between the char gasification rate control and linear pyrolysis rate control around 750 °C. Error bars (not shown) of ± 21 $\text{kg m}^{-2} \text{hr}^{-1}$ represent a 95% confidence interval. b, The form of the cellulose temperature profile is depicted as a function of the rod length. As heat flux, Q_{flux} , from the catalyst through cellulose increases, the thermal gradient increases (becomes sharper). At high heat flux from the surface, Q_{flux} , the sharp temperature gradient permits very little (length b) of the extended cellulose rod to exist within the char-forming temperature range (~ 300 – 400 °C). However, as T_{surface} decreases below ~ 750 °C, Q_{flux} decreases and more of the extended rod (length a) forms char such that char removal by gasification becomes the rate-limiting process.

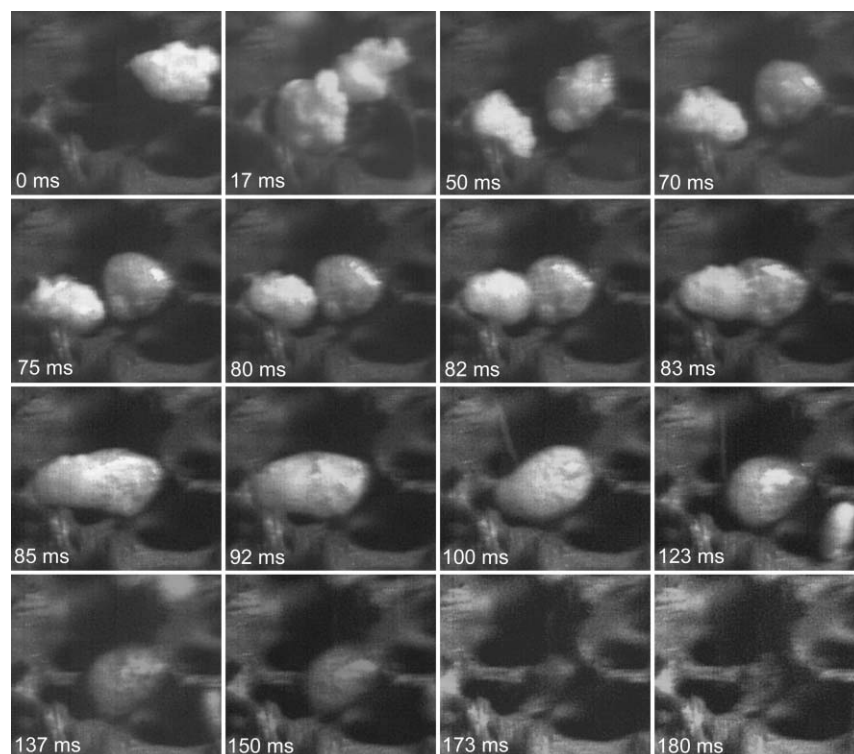


Fig. 4 Millisecond coalescence of cellulose intermediate liquid droplets. Two microcrystalline cellulose particles ($\sim 300\ \mu\text{m}$ each) reacting to volatile species in air on $700\ ^\circ\text{C}$ Rh-Ce/ $\alpha\text{-Al}_2\text{O}_3$ surface have been observed with high-speed photography on an 80 ppi $\alpha\text{-Al}_2\text{O}_3$ foam support at $C/O = 1.15$ from 45° from the surface normal) with temporal resolution of one millisecond. Two particles (coming to rest at 0 and 17 ms) convert to a liquid. The liquid droplets coalesce rapidly (82–85 ms) to a single particle which reactively boils to volatile species observable as gaseous bubbles (100–137 ms) leaving a clean surface (180 ms).

This phenomenon has been observed on catalyst foams when two small particles, each $\sim 300\ \mu\text{m}$, come to rest near each other and decompose to an intermediate liquid during the same period of time as shown in Fig. 4. Within 80 ms of the first particle landing, the particle on the right is fully liquid and the particle on the left is mostly liquid. Within a few milliseconds, the two liquid droplets combine to form a single particle. The most violent motion forming the bridge between the two particles occurs faster than a single millisecond and can only be inferred from the frames and video. The combined particle continues to form a spherical shape in the next 25 ms before completely volatilizing at 180 ms. All frames are available as supplementary video 2.†

The existence of a processing regime capable of combining pyrolysis of biomass particles with catalysis facilitates the development of new reactor designs and chemistries. Many of the conclusions developed here regarding the liquid intermediate, high heat transfer rates, and large particle processing can be extended to previous non-catalytic biomass reactors (e.g. biomass ablative vortex reactor).³⁰ Additionally, new combinations of pyrolysis and catalysis become more viable, including mixed pyrolysis/hydrogenation, pyrolysis/hydrodeoxygenation, or pyrolysis/cracking. However, additional research will be required to more fully describe the solid-nonvolatile fluid heat transfer mechanism as well as the operating parameters that control the large particle regime transition.

Conclusions

High speed photography reveals that direct impingement of microcrystalline cellulose particles with Rh-based reforming catalysts at $700\ ^\circ\text{C}$ produces an intermediate liquid phase that reactively boils to vapors. The intermediate liquid maintains contact with the catalyst surface permitting high heat transfer ($3.4\ \text{MW m}^{-2}$) generating an internal thermal gradient visible within the particle as a wave of solid to liquid conversion. During the period of solid to liquid conversion, the particle height decreased linearly with time. Complete conversion to liquid yields a fluid droplet on the catalyst surface exhibiting linear decrease in droplet volume with time leaving behind a clean surface absent solid residue (char). Under specific interfacial conditions, conversion with large cellulosic particles on the length-scale of wood chips occurs continuously as generated liquid and vapors are pushed into the porous surface.

Acknowledgements

We acknowledge funding from the U.S. Department of Energy and the Initiative for Renewable Energy and the Environment (IREE) at the University of Minnesota. We also acknowledge assistance from Professor Ulrike Tschirner in preparing and analyzing cellulose samples. We also thank Jennifer Dederich for photographic assistance.

References

- 1 G. W. Huber, S. Iborra and A. Corma, Synthesis of Transportation Fuels from Biomass: Chemistry, Catalysts, and Engineering, *Chem. Rev.*, 2006, **106**, 4044–4098.
- 2 NSF, 2008. *Breaking the Chemical and Engineering Barriers to Lignocellulosic Biofuels: Next Generation Hydrocarbon Biorefineries*. Ed. George W. Huber, University of Massachusetts Amherst. National Science Foundation. Chemical, Bioengineering, Environmental, and Transport Systems Division. Washington D.C. 180 p.
- 3 B. C. Gates, G. W. Huber, C. L. Marshall, P. N. Ross, J. Siirola and Y. Wang, Catalysts for Emerging Energy Applications, *MRS Bull.*, 2008, **33**, 429–435.
- 4 A. M. Hansgate, P. D. Schloss, A. G. Hay and L. P. Walker, Molecular characterization of fungal community dynamics in the initial stages of composting, *FEMS Microbiol. Ecol.*, 2005, **51**, 209–214.
- 5 T. R. Carlson, T. P. Vispute and G. W. Huber, Green gasoline by catalytic fast pyrolysis of solid biomass derived compounds, *ChemSusChem*, 2008, **1**, 397–400.
- 6 P. J. Dauenhauer, B. J. Dreyer, N. J. Degenstein and L. D. Schmidt, Millisecond reforming of solid biomass for sustainable fuels, *Angew. Chem., Int. Ed.*, 2007, **46**, 5864–5867.
- 7 J. L. Colby, P. J. Dauenhauer and L. D. Schmidt, Millisecond autothermal steam reforming of cellulose by reactive flash volatilization, *Green Chem.*, 2008, **10**, 773–783.
- 8 G. Varhegyi, E. Jakab and M. J. Antal Jr., Is the Broido-Shafizadeh Model for Cellulose Pyrolysis True?, *Energy Fuels*, 1994, **8**, 1345–1352.
- 9 J. Piskorz, P. Majerski, D. Radlein, A. Vladars-Usas and D. S. Scott, Flash Pyrolysis of Cellulose for Production of Anhydro-Sugars, *J. Anal. Appl. Pyrolysis*, 2000, **56**, 145–166.
- 10 J. Ledé, J. P. Diebold, G. V. C. Peacocke, J. Piskorz, “The Nature and Properties of Intermediate and Unvaporized Biomass Pyrolysis Material”, In: A. V. Bridgwater, D. G. B. Boocock, editors. *Developments in Thermochemical Biomass Conversion*. London: Blackie Academic & Professional; 1997. pp. 27–42.
- 11 C. DiBlasi, Modeling chemical and physical processes of wood and biomass pyrolysis, *Prog. Energy Combust. Sci.*, 2008, **34**, 47–90.
- 12 A. G. W. Bradbury, Y. Sakai and F. Shafizadeh, Kinetic model for pyrolysis of cellulose, *J. Appl. Polym. Sci.*, 1979, **23**, 3271–3280.
- 13 J. P. Diebold, A Unified, Global Model for the Pyrolysis of Cellulose, *Biomass Bioenergy*, 1994, **7**, 75–85.
- 14 A. G. Uden, F. Berruti and D. S. Scott, A Kinetic Model for the Production of Liquids from the Flash Pyrolysis of Biomass, *Chem. Eng. Commun.*, 1988, **65**, 207–221.
- 15 J. Piskorz, D. Radlein and D. S. Scott, On the Mechanism of the Rapid Pyrolysis of Cellulose, *J. Anal. Appl. Pyrolysis*, 1986, **9**, 121–137.
- 16 J. Ledé, H. Z. Li and J. Villermaux, Fusion-Like Behaviour of Wood Pyrolysis, *J. Anal. Appl. Pyrolysis*, 1987, **10**, 291–308.
- 17 O. Boutin, M. Ferrer and J. Ledé, Radiant flash pyrolysis of cellulose—Evidence for the formation of short life time intermediate liquid species, *J. Anal. Appl. Pyrolysis*, 1998, **47**, 13–31.
- 18 D. L. Pyle and C. A. Zaror, Heat Transfer and Kinetics in the Low Temperature Pyrolysis of Solids, *Chem. Eng. Sci.*, 1984, **39**, 147–158.
- 19 C. Di Blasi, Kinetics and Heat Transfer Control in the Slow and Flash Pyrolysis of Solids, *Ind. Eng. Chem. Res.*, 1996, **35**, 37–46.
- 20 A. M. C. Janse, R. W. J. Westerhout and W. Prins, Modelling of flash pyrolysis of a single wood particle, *Chem. Eng. Process.*, 2000, **39**, 239–252.
- 21 A. M. Kanury, Combustion Characteristics of Biomass Fuels, *Combust. Sci. Technol.*, 1994, **97**, 469–491.
- 22 W. E. Ranz and W. R. Marshall Jr., *Chemical Engineering Progress*, 1952, **48**, 141–146; W. E. Ranz and W. R. Marshall Jr., *Chemical Engineering Progress*, 1952, **48**, 173–180.
- 23 I. Milosavljevic, V. Oja and E. M. Suuberg, Thermal Effects in Cellulose Pyrolysis: Relationship to Char Formation Processes, *Ind. Eng. Chem. Res.*, 1996, **35**, 653–662.
- 24 S. Chandra and C. T. Avedisian, Observations of Droplet Impingement on a Ceramic Porous Surface, *Int. J. Heat Mass Transfer*, 1992, **35**, 2377–2388.
- 25 Y. M. Arifin, T. Furuhashi, M. Saito and M. Arai, Diesel and Biodiesel Fuel Deposits on a Hot Surface, *Fuel*, 2008, **87**, 1601–1609.
- 26 J. Ledé, J. Panagopoulos, H. Z. Li and J. Villermaux, Fast pyrolysis of Wood: direct measurement and study of ablation rate, *Fuel*, 1985, **64**, 1514–1520.
- 27 G. V. C. Peacocke and A. V. Bridgwater, Ablative Plate Pyrolysis of Biomass for Liquids, *Biomass Bioenergy*, 1994, **7**, 147–154.
- 28 C. Di Blasi, Heat Transfer Mechanisms and Multi-Step Kinetics in the Ablative Pyrolysis of Cellulose, *Chem. Eng. Sci.*, 1996, **51**, 2211–2220.
- 29 C. Di Blasi, The State of the Art of Transport Models for Charring Solid Degradation, *Polym. Int.*, 2000, **49**, 1133–1146.
- 30 R. S. Miller and J. Bellan, Numerical Simulations of Vortex Pyrolysis Reactors for Condensable Tar Production from Biomass, *Energy Fuels*, 1998, **12**, 25–40.